

# How to Scale-Up Mixing Processes in Non-Newtonian Fluids

**ROBERT J. WILKENS**

UNIV. OF DAYTON

**CHRISTOPHER HENRY**

NORTHWESTERN UNIV.

**AND LEWIS E. GATES**

REYNOLDS INC.

Apply these principles of power-law fluid behavior to scale up mixing processes from the laboratory to the production plant.

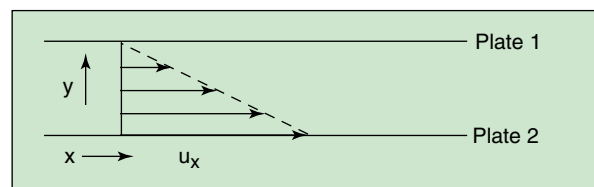
**L**IQUID AGITATION IS A COMMON UNIT operation in the chemical engineering and biological process industries, and its practical use is widely published (1, 2). However, most of the literature on liquid agitation addresses Newtonian fluids, while only limited design information is available on the agitation of non-Newtonian power-law fluids. These fluids are either shear-thinning or shear-thickening — *i.e.*, their apparent viscosity,  $\mu_a$ , decreases (shear-thinning) or increases (shear-thickening) with the shear rate,  $\dot{\gamma}$ .

This article describes the relationships that must be understood in order to scale-up fluid mixing processes in non-Newtonian power-law fluids. The principles described apply to both close-clearance impellers, such as anchors and helixes, and open-turbine impellers.

## Non-Newtonian fluids

It would be ideal to develop a design procedure for general mixer design that would work reliably for all non-Newtonian fluids. However, the prospect of such logic is highly unlikely, due to the complexity and variability of the materials encountered in the process industries. Any design procedure should be verified by actual testing at a scale that is as close to the production scale as possible. The final design of mixers for non-Newtonian power-law fluids should be based on scaleup of successful operating experience.

**Power-law fluids** — Fluids with non-Newtonian characteristics exhibit a non-linear relationship between the shear stress,  $\tau$ , and the shear rate,  $\dot{\gamma}$ . The relationship can be measured with an appropriate viscometer (3). This non-linear behavior can provide some appealing process characteristics. For instance, paints and inks that are highly shear-thinning and have a yield stress can be easily applied using a high shear rate. These materials will not drip or run once they have been applied.



■ Figure 1. Fluid velocity distribution between parallel plates.

Fluid rheology strongly impacts the design of an agitation system. The basics of this subject can be characterized using the steady shear flow between two parallel plates, as illustrated in Figure 1. In this simple flow field,  $\tau$  is the force per area required to maintain Plate 2 in motion at velocity,  $u_x$ , while Plate 1 is held stationary. The shear rate ( $\dot{\gamma}$ ), which is the velocity gradient,  $du_x/dy$ , is proportional to the lower plate velocity when the gap between Plates 1 and 2 is fixed. Newtonian flu-

ids are those for which  $\tau$  and  $\dot{\gamma}$  have a linear relationship:

$$\tau = \mu\dot{\gamma} \quad (1)$$

The proportionality in this relationship,  $\mu$ , is the Newtonian viscosity. It is material-dependent and typically, temperature-dependent. Many fluids exhibit Newtonian behavior, including all gases, liquid metals, low-molecular-weight organic liquids and aqueous solutions of low-molecular-weight solutes (e.g.,  $\text{CaCO}_3$  dissolved in water).

There are many types of non-Newtonian behavior, all of which complicate the analysis of mixing phenomena. Only one of the most common behaviors, that of a power-law fluid, will be analyzed in this article. A power-law fluid exhibits the following relationship between  $\tau$  and  $\dot{\gamma}$ , where  $K'$  and  $n'$  are the material-dependent flow consistency coefficient and flow behavior index, respectively.

$$\tau = K'\dot{\gamma}^{n'} \quad (2)$$

When  $n' = 1$ , the fluid is Newtonian. This relationship can be used to define the apparent viscosity,  $\mu_a$ , of a power-law fluid.

Under shear conditions, a power-law fluid's  $\mu_a$  is:

$$\mu_a = \tau/\dot{\gamma} = K'\dot{\gamma}^{n'-1} \quad (3)$$

When  $n' < 1$ ,  $\mu_a$  decreases with increasing  $\dot{\gamma}$ , and the fluid is termed shear-thinning (or pseudoplastic). For a shear-thinning fluid,  $\tau$  increases with increasing  $\dot{\gamma}$ . However, as shown in Figure 2, the rate of increase is less than linear. This is the most common non-Newtonian behavior, often occurring in polymer melts and biological fluids:

When  $n' > 1$ ,  $\mu_a$  increases with increasing  $\dot{\gamma}$ , and the fluid is termed shear-thickening (or dilatant). For a shear-thickening fluid in Figure 1,  $\tau$  increases faster than linearly with increasing  $\dot{\gamma}$ . This behavior is also depicted in Figure 2. Shear-thickening behavior is most often observed with concentrated slurries, such as titanium dioxide and starch pastes. One explanation is that at rest and low shear rates, there is enough liquid present in the void space between solid particles to prevent the particle-particle interactions that lead to greater friction and an increase in  $\mu_a$ . However, at higher shear rates, the suspension expands (dilates), such that the amount of liquid present cannot overcome the frictional forces between the particles and the consequent increase in  $\mu_a$ .

The non-Newtonian fluids discussed in this article are the simplest of many complex behaviors, and do not include yield stresses, time dependence or elastic phenomena. Chhabra and Richardson (4) provide a thorough review of non-Newtonian rheology.

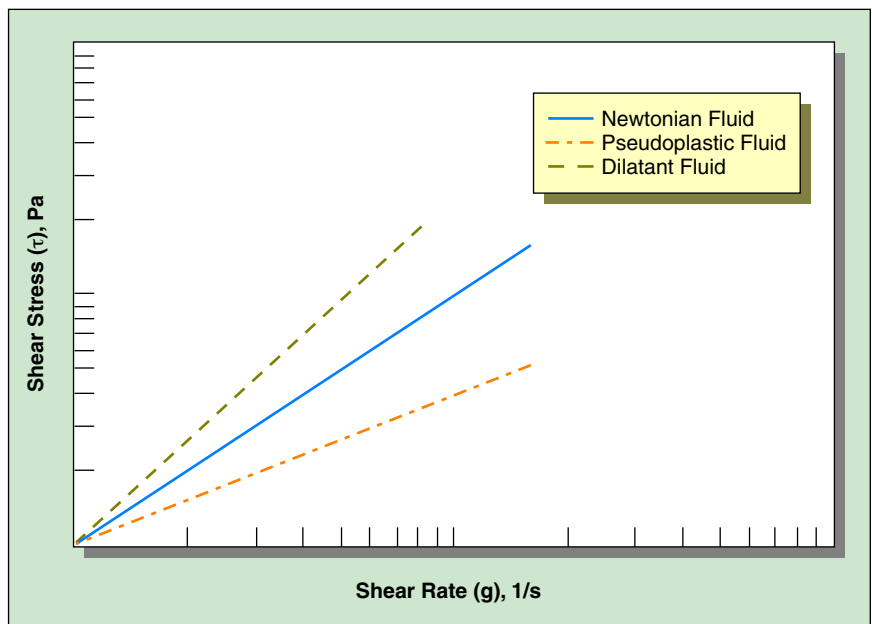
Although the power-law model is an attempt to curve-fit real data with a simple mathematical relationship, it is nonetheless useful in the engineering sense. For instance, most shear-thinning fluids behave in a Newtonian manner (i.e., their viscosity is independent of  $\dot{\gamma}$ ) at very high and very low shear rates (4). Yet, little data spanning the complete range of shear rates is available and typically cannot be obtained using a single rheological device.

Thus, power-law model parameters may only be applicable over a few orders of magnitude of  $\dot{\gamma}$ . Care must be taken to ensure that data should correspond to  $\dot{\gamma}$  encountered during processing.

### How does non-Newtonian behavior affect agitation?

Relating the simple, steady shear flow of Figure 1 to the flow field in an agitated vessel is no simple task. The primary complication is that the flow field in an agitated vessel, including  $\dot{\gamma}$ , is a function of position, and in many cases, time. Therefore, for non-Newtonian liquids,  $\mu_a$  will also depend on time and position within the mixed vessel.

The highest values of  $\dot{\gamma}$  in an agitated vessel occur near the impeller at points of highest local velocity,  $v$ . For open-turbine impellers,  $v$  and  $\dot{\gamma}$  are highest at the impeller tip;  $\dot{\gamma}$  decreases with increasing distance from the impeller and is lowest at the vessel wall. Therefore, shear-thinning liquids will have their lowest  $\mu_a$  in the impeller region of an open



■ Figure 2. Power-law fluid response to shear.

turbine. With close-wall-clearance impellers, such as helical ribbons, shear-thinning fluids will have the lowest  $\mu_a$  near the vessel wall. Common industrial open-turbine and close-clearance impellers are shown in Ref. 2.

For open-turbine impellers, cavern formation may occur in power-law fluids (5, 6). In these caverns, liquid near the impeller will have motion. Pilot studies will indicate whether this motion is sufficient to achieve process objectives. The liquid farther from the impeller and out of the cavern may have very low, or even negligible velocities (7).

Because of the many complications that arise from non-Newtonian fluids, this article assumes that mixing or agitation must have been conducted successfully at a laboratory scale (*i.e.*, Scale 1). The requirement, then, is to predict the intensity of mixing that is required in production (*i.e.*, Scale 2) to duplicate the process result that was observed in Scale 1. Figures 3 and 4 illustrate Scales 1 and 2, respectively.

First the assumption of geometric similarity will be made. Geometric similarity is achieved in Scale 2 by making the ratio of all linear dimensions in Scale 2 identical to those in Scale 1. Figures 3 and 4 are geometrically similar. In mixing scaleup, the objective is to predict the rotational shaft speed in Scale 2 (or  $n_2$ ), that will duplicate the performance measured or observed in Scale 1 as a result of rotational shaft speed in Scale 1 (or  $n$ ).

## Effective impeller shear rate

The fluid's  $\gamma$  varies throughout the volume of the tank. Because of this,  $\mu_a$  also varies. For power-law fluids, Metzner and Otto (8) suggest using an effective shear rate,  $\gamma_{eff}$ , to obtain an effective viscosity for the agitated tank:

$$\gamma_{eff} = k_s n \quad (4)$$

Bakker, *et al.* (7) suggest the use of impeller constants in Table 1 to evaluate  $\gamma_{eff}$  for a wide variety of impellers. Substituting  $\gamma_{eff}$  in Eq. 3 for the particular fluid gives  $\mu_{eff}$ , which can then be used to calculate the impeller Reynolds

## Nomenclature

|             |   |
|-------------|---|
| $b$         | = cavern model parameter, m   |
| $C$         | = height of the impeller (or shaft) above the vessel floor, m                           |
| $D$         | = diameter of the impeller, m   |
| $D_c$       | = cavern diameter, m  |
| $D/T$       | = relative impeller diameter, dimensionless   |
| $D_c/T$     | = relative cavern diameter, dimensionless   |
| $du_x/dy$   | = velocity gradient   |
| $F$         | = total impeller force, N   |
| $F_{ax}$    | = impeller axial force, N   |
| $F_0$       | = impeller tangential force, N  |
| $Fr$        | = Froude number   |
| $g$         | = gravity, m/s <sup>2</sup>   |
| $K'$        | = flow consistency coefficient of a power-law fluid, (N/m <sup>2</sup> )s <sup>n'</sup> |
| $k_s$       | = effective shear rate constant   |
| $N_B$       | = blend number, dimensionless   |
| $N_F$       | = force number, dimensionless   |
| $N_p$       | = power number, dimensionless   |
| $N_Q$       | = pumping number, dimensionless   |
| $n$         | = rotational shaft speed, rev/s   |
| $n_2$       | = rotational shaft speed in Scale 2, rev/s  |
| $n'$        | = flow behavior index of a power-law fluid  |
| $P$         | = impeller power, W   |
| $P_i$       | = pitch of a helical ribbon impeller, m   |
| $P_M$       | = minimum motor power, W  |
| $q$         | = theoretical impeller pumping rate, m <sup>3</sup> /s                                  |
| $Re_n$      | = Reynolds number for a power-law fluid, dimensionless                                  |
| <i>s.g.</i> | = specific gravity, dimensionless   |
| $S_t$       | = impeller tip speed, m/s   |
| $t$         | = impeller torque, N-m  |
| $T$         | = tank diameter, m  |
| $u_x$       | = velocity of lower plate at a certain shear rate, m/s                                  |
| $V$         | = volume, m <sup>3</sup>  |
| $v$         | = local fluid velocity, m/s   |
| $v_{bf}$    | = bulk fluid velocity, m/s  |
| $v_o$       | = cavern boundary velocity, m/s   |
| $Z$         | = depth of the liquid in a vessel, m  |

## Greek Letters

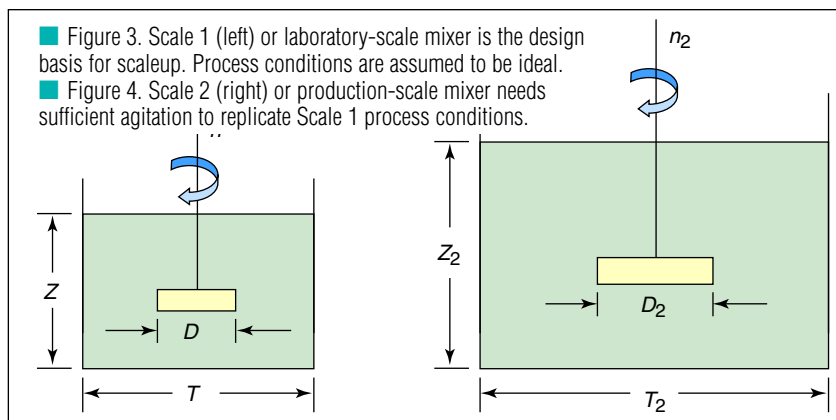
|                |   |
|----------------|---|
| $\gamma$       | = shear rate, 1/s   |
| $\gamma_{eff}$ | = effective shear rate, 1/s                                       |
| $\mu$          | = absolute or dynamic viscosity, Pa-s                             |
| $\mu_a$        | = apparent viscosity for a power-law fluid, Pa-s (Eq. 3)          |
| $\mu_{eff}$    | = effective dynamic viscosity for a power-law fluid, Pa-s (Eq. 5) |
| $\theta$       | = blend time, s   |
| $\rho$         | = density, kg/m <sup>3</sup>                                      |
| $\tau$         | = shear stress, N/m <sup>2</sup> (Eqs. 1 and 2)                   |

number for power-law fluids,  $Re_n$ :

$$\mu_{eff} = \tau / \gamma_{eff} = K' (k_s n)^{n'-1} \quad (5)$$

## Impeller performance characteristics database

There are several important dimensionless numbers that are required to design mixers. All must be determined experimentally for a given impeller configuration. These numbers can be used to quantify the performance characteristics of an impeller. Dimensionless numbers are affected by geometric factors, such as the ratio of im-



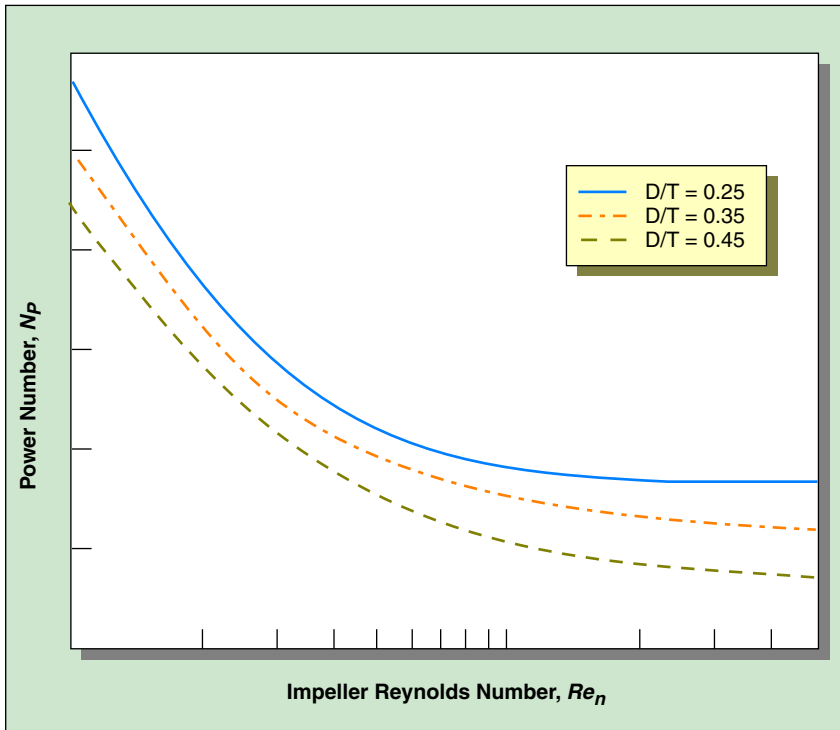


Figure 5.  $N_p$  is inversely proportional to  $Re_n$  in the laminar and transitional flow regimes and becomes constant in the turbulent regime.

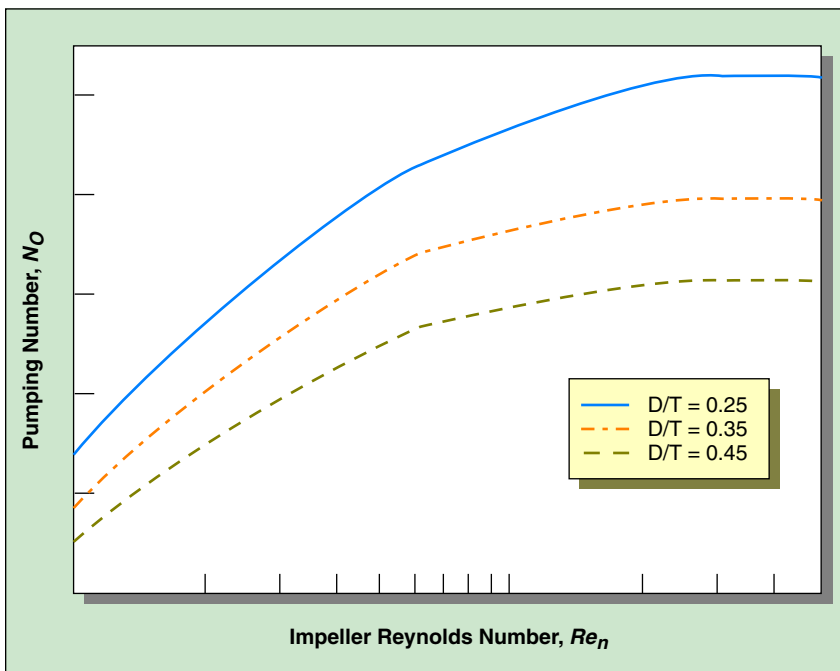


Figure 6.  $N_Q$  generally increases with  $Re_n$  in the laminar and transitional flow regimes and becomes constant in the turbulent regime.

impeller to tank diameter,  $D/T$ , and the ratio of clearance from the tank bottom to tank diameter,  $C/T$ . All these dimensionless parameters are normally correlated against  $Re_n$  for a baffled tank.

The impeller blend number,  $N_B$ , is used to predict the blend time,  $\theta$ , in a mixed system.  $N_B$  attempts to predict the effect of impeller  $D/T$  on the results:

$$N_B = n\theta(D/T)^{2.3} \quad (6)$$

The impeller power number,  $N_p$ , is used to predict impeller power,  $P$ , directly and torque,  $t$ , indirectly:

$$N_p = P/\rho n^3 D^5 \quad (7)$$

The impeller pumping number,  $N_Q$ , is used to predict the impeller pumping rate,  $q$ , directly and the bulk fluid velocity,  $v_{bf}$ , indirectly:

$$N_Q = q/nD^3 \quad (8)$$

The impeller force number,  $N_F$ , correlates the axial force,  $F_{ax}$ , or the thrust generated by an impeller.  $F_{ax}$  is used in the correlation to predict cavern dimensions and is also important to mechanical design considerations:

$$N_F = F_{ax}/\rho n^2 D^4 \quad (9)$$

Finally,  $Re_n$  for power-law fluids measures the ratio of inertial to viscous forces within the mixing environment:

$$Re_n = \rho n D^2 / (k_s n)^{n-1} \quad (10)$$

As stated previously, all of the dimensionless numbers just discussed are correlated with  $Re_n$ .

Examples of the correlations for  $N_p$ ,  $N_B$ ,  $N_Q$  and  $N_F$  are given in Figures 5–8. These correlations depict the trends observed for axial-flow impellers, such as pitched-blade or high-efficiency turbines, for different values of  $D/T$ . Note the sudden drop in  $N_F$  (Figure 8) when turbulent flow is reached.

While there is considerable information in the literature about these dimensionless numbers, no single reference provides a complete picture. The authors

have assembled an extensive database of impeller performance parameters for scaleup. This database was stored as individual data points in a text file. In order to find values of the dimensionless numbers between data points of impeller performance parameters, an interpolation algorithm is used. With this library,  $N_p$ ,  $N_B$ ,  $N_Q$  and  $N_F$  are available for a variety of common industrial impeller types.

## Scaleup criteria

The scaleup criteria discussed in this article are based on the assumption that Scale 1 and Scale 2 are geometrically similar, and that Scale 2 is larger than Scale 1. Scaleup criteria will be discussed in the order of increasing conservatism in mixer design (*i.e.*, mixer size will be increasing as Scale 1 is converted to Scale 2 for the subsequent criteria). A sample scaleup is performed later in this article.

**Equal Reynolds number** — Holding  $Re_n$  fixed with scaleup results in the smallest production mixer of any of the criteria discussed in this paper. For this reason, scaleup based on equal  $Re_n$  is not usually recommended.

**Equal relative cavern diameter** — Wichterle, *et al.* (9), who studied pseudoplastic and plastic suspensions of finely divided particulate solids, used the term “cavern” to describe the well-mixed, turbulent region around the impeller. Amanullah, *et al.* (6) proposed an axial-force model for predicting the cavern diameters,  $D_c$ , in highly shear-thinning liquids using axial-flow impellers:

$$D_c = [4v_o(2/n' - 1)(4\pi^2K'/F)^{1/n'} + b(n' - 2)^{1/n'}]^{n'/(n' - 2)} \quad (11)$$

where  $b = T/4$  (12)

$$F = (F_{ax}^2 + F_{\theta}^2)^{1/2} \quad (13)$$

$$F_{\theta} = 8t/3D \quad (14)$$

$F_{ax}$  is derived from Eq. 9 and

$$t = N_p \rho n^2 D^5 / 2\pi \quad (15)$$

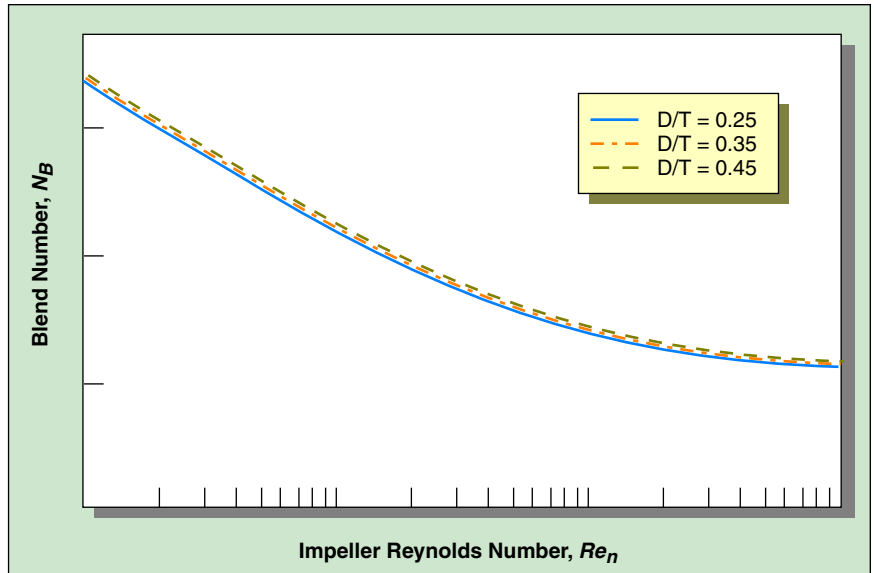


Figure 7.  $N_B$  is inversely proportional to  $Re_n$  in the laminar and transitional flow regimes and becomes constant in the turbulent regime.

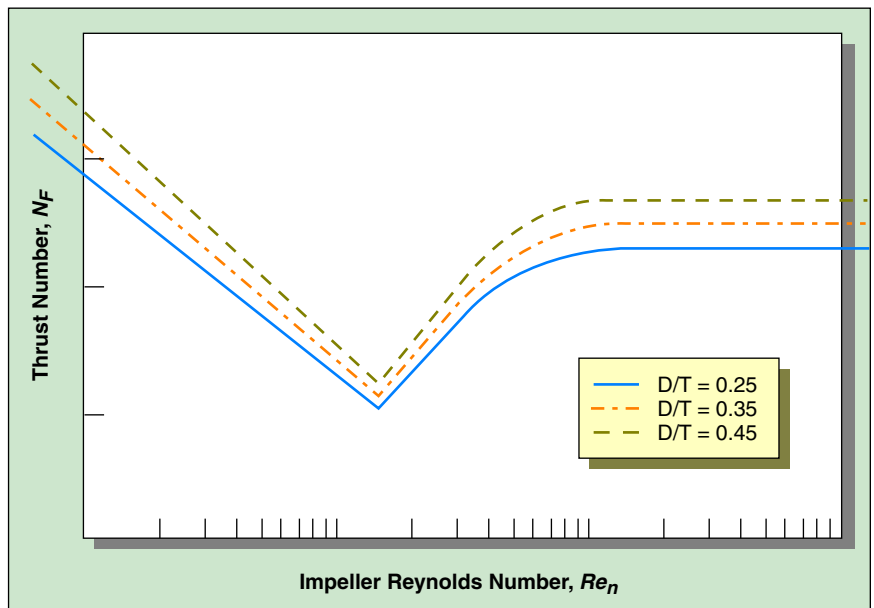
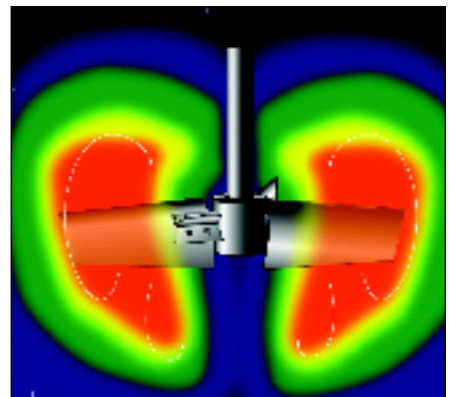


Figure 8.  $N_F$  decreases with  $Re_n$  in the laminar and transitional flow regimes, and suddenly increases before fully turbulent flow is reached.

Figure 9.

Shown is the flow pattern created by a high-efficiency impeller rotating in a power-law fluid. Red shows areas of high velocity. Blue shows areas that are stagnant or that have very low velocities. Courtesy of Denise Minch, graphic artist (DeniseMinch@hotmail.com).



In principle, Eq. 11 can also be used to predict the size of caverns generated by radial-flow impellers. It shows that scaleup based on equal relative cavern diameter,  $D_c/T$ , results in production mixers for Scale 2 that are slightly larger than those suggested by scaleup based on equal  $Re_n$ .

Although fluid in the cavern is highly mobile, further away from the impeller, where shear stresses are below the yield stress, the fluid may be stagnant. It is possible to increase the size of the cavern by increasing the impeller diameter or speed (Figure 9). The authors recommend that  $D_c$  of mixed regimes be evaluated, but they do not recommend the use of  $D_c/T$  as a scaleup mechanism.

**Equal tip speed** — The impeller tip speed,  $S_t$ , is a common scaleup criterion for industrial mixers, often associated with shear-sensitive mixing phenomena, such as particle- or droplet-size control:

$$S_t = \pi n D \quad (16)$$

The authors recommend that equal  $S_t$  be used as a scaleup criterion only when small-scale studies have clearly shown that desirable process performance correlates with  $S_t$ . One example might be when  $S_t$  has proven to be an important predictor of desirable product turbidity for a liquid product, or desirable particle-size distribution in a slurry.

**Equal torque per volume** — Torque per volume,  $t/V$ , is a measure of torque invested by a fluid mixer per unit of mixed volume. It is calculated as the ratio of  $t$  (from Eq. 15) to  $V$ , defined as:

$$V = \pi T^2 Z / 4 \quad (17)$$

$t/V$  is a practical and common scaleup criterion for fluid mixers because it relates directly to the size and torque capability of the mixer.

**Equal bulk fluid velocity** — Bulk fluid velocity,  $v_{bf}$ , is often used as a scaleup parameter in low-viscosity applications:

$$v_{bf} = 4q / \pi T^2 \quad (18)$$

In Eq. 18,  $q$  is the volumetric flowrate of the fluid leaving the impeller blades and  $\pi T^2 / 4$  is the cross-sectional area of the tank. In addition, it can be shown that equal  $S_t$ , equal  $t/V$  and equal  $v_{bf}$  are identical for turbulent-flow conditions in Newtonian fluids when geometric similarity is maintained.

**Equal power per volume** — Scaleup based on equal power per volume,  $P/V$ , is probably the most commonly used criterion in mixing because it is easily understandable and practical. To calculate  $P/V$ , rearrange Eq. 7 to solve for  $P$ :

$$P = N_p \rho n^3 D^5 \quad (19)$$

and calculate  $V$  using Eq. 17. Other advantages of using

**Table 1.  $k_s$  values for effective shear rate ( $\gamma_{eff}$ ) model (Eq. 5, Ref. 7).**

| Impeller Type                              | $k_s$ |
|--|-------|
| High-efficiency                            | 10    |
| Pitched-blade                              | 11    |
| Straight-blade                             | 11    |
| Disc-turbine                               | 11.5  |
| Anchor ( $D/T = 0.98$ )                    | 24.5  |
| Helical-ribbon ( $D/T = 0.96, P_i/D = 1$ ) | 29.4  |

The values for the anchor and helical ribbon impellers are for the specified standard geometries only. For other geometries, use:  $\gamma_{eff} = 25 (D/T)^{1/2} [P_i(p^2 D^2 + P^2)^{1/2}]^{-0.152} n$  and  $\gamma_{eff} = 25 (D/T)^{1/2} n$  for anchor and helical ribbon impellers, respectively.

$P/V$  as a scaleup criterion are that it correlates well with mass-transfer characteristics in the mixer, and it is conservative enough to provide adequate performance in production-scale equipment — particularly when no other strong correlating parameter has been determined from small-scale testing. The authors recommend  $P/V$  as a scaleup criterion when no others are obvious.

**Equal Froude number** — The Froude number,  $Fr$ , is the ratio of inertial to gravitational force:

$$Fr = n^2 D / g \quad (20)$$

Rotational speed tends to decrease with most scaleup criteria. As shown in Eq. 20,  $n$  will have a powerful, non-linear effect on  $Fr$ , causing  $Fr$  to decrease with increasing volume, even though  $D$  is increasing. Thus, scaleup based on equal  $Fr$  is rarely used as a scaleup criterion because it results in a relatively large and expensive industrial mixer.

**Equal blend time** — Because blend time,  $\theta$ , increases with increasing tank volume, maintaining equal  $\theta$  with scaleup is difficult and expensive — so much that the selection of equal  $\theta$  as a scaleup criterion is often considered impractical.

$$\theta = N_B / (n(D/T)^{2.3}) \quad (21)$$

However, a moderate increase in  $\theta$  in the large vessel may reduce the power and torque requirements to a more acceptable level from a cost perspective. Such tradeoffs are often made in order to purchase agitation equipment of reasonable size (2). If equal  $\theta$  is an absolute design criterion, economics will dictate how large the production-scale mixer shall be.

## From process design to production

A mixer design procedure must enable the user to specify the critical components of mixer construction. The critical components of a fluid mixer are the motor, drive (speed reducer or torque increaser), shaft and impeller.

**Mixer motor** — The motor provides the power to drive the impellers in the process fluid at speeds required to deliver the desired process result. The motor must also pro-

vide additional power for losses that occur in mixer drives, seals and couplings. One must also plan for process upsets and process-fluid variability. After accounting for all power requirements, one should select the next-largest available motor from a database of mass-produced motors so that costs are controlled.

**Mixer drive** — The mixer drive must be designed for the maximum torque required by the impeller system, whether the mixer is in start-up or at steady-state operation. At startup, the low shear rates produced by the impeller will create high  $\mu_{eff}$  in a shear-thinning fluid. At steady-state conditions, the mixer drive transmits power, reduces motor speed and increases torque. In addition, the drive bearings normally support the mixer shaft and impeller system.

To specify a drive that will have sufficient torque for the application, the user should select the American Gear Manufacturers Assn. (AGMA) speed that is just below the calculated operating speed. Selecting the next-lower AGMA speed for drive increases the torque of the drive, and is therefore conservative. The combination of higher power and lower motor speed will require an impeller that is larger than the geometrically similar impeller used as the basis for calculations. This larger impeller will effectively improve the final mixer performance.

**Mixer shaft** — The mixer shaft transmits power to the impeller and must be designed properly for torque, bending moments and natural vibration frequencies. The calculations required for shaft design are complex and beyond the scope of this paper. Detailed coverage is provided in Ref. 10. Users should seek the expertise of consultants or mixer manufacturers when performing calculations for shaft design.

**Mixer impeller** — After selecting the most appropriate impeller configuration (e.g., axial, radial, pitch-blade, high-efficiency, helical-ribbon, etc.) for Scale 1, a geometrically similar impeller should be chosen for Scale 2. The mixer impeller must be properly sized to transmit the power and torque from the motor to the process fluid for proper function. Many of the mechanical design specifications required to completely design a fluid mixer are beyond the scope of this paper. In this article, the emphasis is on the specification of the motor horsepower, the mixer shaft speed, impeller configuration and impeller size for proper process function. The complete mechanical design of the fluid mixer should be left to manufacturers experienced in that design technology.

## Algorithm for scale-up of power-law fluids

The necessary calculation sequence for scale-up of mixing phenomena in power-law fluids must consider the following physical conditions: Any impeller rotating in a fluid will shear the fluid; the  $\gamma_{eff}$  of the impeller must be determined. The induced shear alters the  $\mu_a$  of the fluid as dictated by power-law parameters. Thus,  $\mu_{eff}$  is used to calcu-

## Scaleup Algorithm

### Step I. Define successful small scale (Scale 1) conditions

- Measure the power-law characteristics of the fluid viscosity
  - measure the fluid properties s.g.,  $K'$  and  $n'$
- Measure the system geometry of Scale 1
  - measure  $C, D, T$  and  $Z$
  - calculate  $V$  (Eq. 17),  $D/T$  and  $Z/T$
- Define the impeller style used in Scale 1
  - find  $k_s$  for the specified impeller (e.g., disc, pitched-blade, high-efficiency, helical-ribbon, etc.)
- Find the optimum operating conditions
  - observe  $n$
- Calculate the  $Re_n$  of successful conditions in Scale 1 (Eq. 10)
- Look up  $N_B, N_F, N_Q$  and  $N_P$  for that calculated  $Re_n$  and for the geometry ( $C/T, D/T$ , etc.) in Scale 1
- Calculate  $\mu_{eff}$  (Eq. 5)
- Calculate  $F_{ax}, F_{\theta}$ , and  $F$  (Eqs. 9, 13 and 14)
  - select  $v_o$
  - calculate  $D_c$  (Eq. 11)
- Calculate  $D_c/T$
- Calculate  $P$  (Eq. 19)
- Calculate  $P_M$  ( $P_M = P/0.85$ )
- Calculate  $t$  (Eq. 15)
- Calculate  $P/V$  and  $t/V$
- Calculate  $Fr$  (Eq. 20)
- Calculate  $S_t$  (Eq. 16)
- Calculate  $v_{bf}$  (Eq. 18)
- Calculate  $\theta$  (Eq. 21)
- Output results to a spreadsheet for later comparison.

### Step II. Define Scale 2

- Calculate the system geometry of Scale 2 from Scale 1 and geometric similarity.
- Calculate  $n_2$  required to produce  $Re_n$  of Scale 1
- Calculate  $\mu_{eff}$
- Calculate  $D_c/T$
- Calculate  $P$
- Calculate  $P_M$
- Calculate  $t$
- Calculate  $P/V$  and  $t/V$
- Calculate  $Fr$
- Calculate  $S_t$
- Calculate  $v_{bf}$
- Calculate  $\theta$
- Output the results to a spreadsheet or database
- Compare the calculated characteristics in Scale 2 to Scale 1
- Repeat the calculations in Step II, incrementing  $Re_n$ , (and thus,  $n_2$ ) and updating  $N_B, N_F, N_Q$  and  $N_P$  (Eqs. 6–9).

### Step III. Compare the results until the desired characteristics of Scale 2 match those of Scale 1.

### Step IV. Specify a motor and a mixer drive.

Table 2. Summary of sample scale-up analysis.

| Column 1                              | Column 2     | Column 3 | Column 4 | Column 5 | Column 6 | Column 7          |
|---------------------------------------|--------------|----------|----------|----------|----------|-------------------|
|                                       | Scale 1      | Scale 2  | Scale 2  | Scale 2  | Scale 2  | Scale 2           |
| Scaleup Basis                         | Base         | Equal    | Equal    | Equal    | Equal    | Equal             |
|                                       | Condition    | $Re_n$   | $T/V$    | $P/V$    | $Fr$     | Relative $\theta$ |
| $V$ , gal                             | 20           | 1,000    | 1,000    | 1,000    | 1,000    | 1,000             |
| $D/T$                                 | 0.33         | 0.33     | 0.33     | 0.33     | 0.33     | 0.33              |
| <i>s.g.</i>                           | 1            | 1        | 1        | 1        | 1        | 1                 |
| $n'$                                  | 0.224        | 0.224    | 0.224    | 0.224    | 0.224    | 0.224             |
| $K'$ , $N\text{-m}^{-2}\text{s}^{n'}$ | 40           | 40       | 40       | 40       | 40       | 40                |
| $n$ , rev/min                         | 244          | 57       | 71       | 109      | 127      | 244               |
| $T$ , in.                             | 18.1         | 66.5     | 66.5     | 66.5     | 66.5     | 66.5              |
| $Z$ , in.                             | 18.1         | 66.5     | 66.5     | 66.5     | 66.5     | 66.5              |
| $D$ , in.                             | 5.96         | 21.9     | 21.9     | 21.9     | 21.9     | 21.9              |
| $S_p$ , ft/min                        | 380          | 327      | 408      | 626      | 730      | 1402              |
| $P$ , hp                              | 0.0329       | 0.283    | 0.486    | 1.65     | 2.63     | 20.3              |
| $P_M$ , hp                            | 0.0387       | 0.333    | 0.571    | 1.95     | 3.1      | 23.9              |
| $t$ , in-lb <sub>f</sub>              | 10           | 368      | 507      | 1,125    | 1,537    | 6,182             |
| $t/V$ , in-lb <sub>f</sub> /1,000 gal | 500          | 368      | 507      | 1,125    | 1,537    | 6,182             |
| $P/V$ , hp/1,000 gal                  | 1.93         | 0.333    | 0.571    | 1.95     | 3.1      | 23.9              |
| $N_p$                                 | 4.61         | 4.58     | 4.07     | 3.83     | 3.85     | 4.2               |
| $N_F$                                 | 0            | 0        | 0        | 0        | 0        | 0                 |
| $Fr$                                  | 0.256        | 0.0516   | 0.08     | 0.189    | 0.256    | 0.945             |
| $Re_n$                                | 48           | 49       | 72       | 154      | 202      | 645               |
| $\mu_{eff}$ , cP                      | 1,959        | 6,052    | 5,104    | 3,659    | 3,250    | 1,958             |
| $D_c$ , in                            | 17.7         | 65.1     | 66.1     | 66.5     | 66.5     | 66.5              |
| $D_c/T$                               | 0.980        | 0.979    | 0.995    | 1.00     | 1.00     | 1.00              |
| Relative $\theta'$                    | 1 (assigned) | 4.3      | 3.4      | 2.2      | 1.9      | 1.0               |
| Recommended shaft speed, rev/min      | 190          | 56       | 68       | 100      | 125      | 190               |
| Recommended motor power, hp           | 0.25         | 0.5      | 0.75     | 2        | 5        | 25                |

\* Blend times in Columns 2–7 are relative to Scale 1.

late  $Re_n$  in order to determine  $N_B$ ,  $N_F$ ,  $N_p$  and  $N_Q$  of the impeller system at those conditions.  $N_B$ ,  $N_F$ ,  $N_p$  and  $N_Q$  are variable and are correlated against  $Re_n$  and the system geometry (Figures 5–8). For a given impeller  $n$ , solve for  $P$ ,  $t$ ,  $q$  and  $\theta$ . This design procedure requires iterative calculations described in the sidebar algorithm.

### Scaleup example

Scale 1 is a 20-gal pilot reactor with a six-bladed Rushton disc impeller with a 5.96-in. dia. It is important to note that the axial force produced by a Rushton impeller, or by any other radial-flow impeller, is effectively zero, so that  $N_F = 0$  for all conditions studied in Scale 1.

The process fluid is a shear-thinning power-law fluid with  $K' = 40 \text{ N}\cdot\text{m}^{-2}\text{s}^{n'}$  and  $n' = 0.224$ . After numerous runs, it is determined that the optimum process performance is achieved at  $n = 244 \text{ rev/min}$ . The performance conditions in the 20-gal reactor are summarized in Column 2 of Table 2.

The planned production size of Scale 2 is 1,000 gal. The objective is to select conditions in Scale 2 that will provide equivalent performance to that observed in Scale 1. There is no one parameter in mixed systems that will assure success in scaleup. The authors recommend looking at a variety of parameters expected to influence performance (e.g.,  $S_p$ ,  $P/V$ ,  $t/V$ , etc.) and then to use the cal-

culated values of those parameters from Scale 1 as a database from which to select the final mixing conditions in Scale 2.

The authors developed a computer program based on the algorithm discussed in this article to facilitate the analysis of mixer scaleup. The program starts the analysis at a shaft speed specified by the user and increments to a maximum shaft speed, also provided by the user. The calculated information for each speed is exported to a file that can be read by Excel or by another equivalent software. The information is then summarized in a spreadsheet where it can be studied in order to select the appropriate scaleup parameters.

Table 2 contains the scaleup calculation summary for the 1,000-gal Scale 2 in Columns 3–7. Notice that each successive scaleup criterion results in a  $n$  that is higher than the previous criterion. The result is a bigger mixer with higher torque, higher first cost and higher running costs (reflected by power requirement), as expected.

While the authors generally recommend a  $P/V$  scaleup criterion when no other criterion is obvious, Table 2 illustrates that relative  $\theta$  for the  $P/V$  column is 2.2 times greater than the equal relative  $\theta$  scaleup shown in the last column. This compromise must be considered versus the higher costs of the mixer designed on the basis of equal  $\theta$ .

The equations defined in this article are presented in SI

units instead of English units, because the latter would require correction factors to make certain formulas dimensionless. However, the example problem uses English units (*e.g.*,  $P/V$  is defined in hp/1,000 gal) with the understanding that most of readers would prefer to analyze the problems in those terms.

## Conclusions

Scaleup of mixing in power-law fluids is complicated because  $\mu_a$  varies with  $\gamma$ . Changes in the  $\mu_a$  can shift the  $Re_n$  into the transitional or laminar flow regimes, which, as illustrated in Figures 5–8, causes a change in  $N_B$ ,  $N_P$ ,  $N_Q$  and  $N_F$ . The solution to the equations involved for power-law fluids becomes a trial-and-error process.

The design logic described in this article depends on having reliable values of  $N_B$ ,  $N_P$ ,  $N_Q$  and  $N_F$  over the laminar, transitional and turbulent flow regimes for the impeller system being analyzed. Often, data are unavailable from a single source. But, once obtained, these data allow selection of the appropriate scaleup criterion, ultimately leading to successful scaleup of power-law fluid agitation.

CEP

## Literature Cited

1. Brodkey, R. S. and H. Hershey, "Transport Phenomena: A Unified Approach," McGraw-Hill, New York, NY, pp. 359–399 and pp. 752–790 (1988).
2. McCabe, W. L., *et al.*, "Unit Operations of Chemical Engineering, Sixth Ed.," McGraw-Hill, New York, NY, pp. 238–285 (2001).
3. ASTM D4040-99, "Standard Test Method for Viscosity of Printing Inks and Vehicles by the Falling-Rod Viscometer," (1999).
4. Chhabra, R. P. and J. F. Richardson, "Non-Newtonian Flow in the Process Industries," Butterworth Heinemann, Boston, MA (1999).
5. Nienow, A. W. and T. P. Elson, "Aspects of Mixing in Rheologically Complex Fluids," *Chemical Engineering Research & Design*, Dept. of Chem. Eng., The Univ. of Birmingham, U.K., **66** (1988).
6. Amanullah, A., *et al.*, "A New Mathematical Model to Predict Cavern Diameters in Highly Shear Thinning Power Law Liquids Using Axial Flow Impellers," Centre for Bioprocess Engineering, School of Chem. Eng., The Univ. of Birmingham, Birmingham, U.K.; *Chem. Eng. Science*, **53** (3), pp. 455–469 (1998).
7. Bakker, A. and L. E. Gates, "Properly Choose Mechanical Agitators for Viscous Liquids," *Chem. Eng. Prog.*, **91** (12), pp. 25–34 (Dec. 1995).
8. Metzner, A. B. and R. E. Otto, "Agitation of Non-Newtonian Fluids," *AIChE J.*, **3** (1), pp. 3–10 (1957).
9. Wichterle, K. and O. Wein, Paper B4.6, International Congress of Chemical and Process Engineering, CHISA '75, Prague, Czech Republic (1975).
10. Fasano, J. B., *et al.*, "Consider Mechanical Design of Agitators," *Chem. Eng. Prog.*, **91** (8), pp. 60–71 (Aug. 1995).

## Related Course Offered by AIChE

Course #090: Industrial Fluid Mixing

Member fee: \$995, Non-member fee: \$1,155

Houston, TX; October 27–28, 2003

For more information or to register, visit [www.aiche.org/education](http://www.aiche.org/education) or call (800) 242-4363. Onsite courses are also available.

**ROBERT J. WILKENS** is an assistant professor of chemical engineering at the Univ. of Dayton (300 College Park, Dayton, OH 45469-0246; Phone: (937) 229-2627; Fax: (937) 229-3433; E-mail: [wilkens@udayton.edu](mailto:wilkens@udayton.edu)). His research interests lie in fluid mechanics (agitation and pipe flow), namely, impeller performance and multiphase drag reduction. Wilkens is also the author of several papers in these areas. He holds bachelor and master degrees from the Univ. of Dayton and a PhD from Ohio Univ., all in chemical engineering, and has held a post-doctorate research engineering position at Shell Westhollow Technology Center (Houston, TX). He is a registered professional engineer in Ohio.

**CHRISTOPHER HENRY** is currently pursuing his doctorate at Northwestern Univ. (1311 Chicago Ave, Apt. 204; Evanston, IL 60201; Phone: (847) 467-6720; E-mail: [c-henry@northwestern.edu](mailto:c-henry@northwestern.edu)), having earned a BSChE from Univ. of Dayton (OH) in May 2002. During his time as an undergraduate student, Henry worked for International Papers, where he conducted development work for ink-jet coatings. His current research is in bioinformatics.

**LEWIS E. GATES** is president of ReyNo Inc. (921 Howard Lane, Vandalia, OH 45377; Tel: (937) 264-4112; E-mail [lewisgates@reynoinc.com](mailto:lewisgates@reynoinc.com)), where he develops products, software and application procedures for manufacturers and users of process equipment, while focusing primarily on fluids mixing. After receiving both BS and MS ChE degrees from the Ohio State Univ., Gates worked for DuPont and Chemineer before launching ReyNo, Inc. He is a member of AIChE and a registered professional engineer in the state of Ohio. ReyNo funded the work upon which this paper is based.